IEEE Access
Multidisciplinary | Rapid Review | Open Access Journal

Received December 31, 2018, accepted January 28, 2019, date of publication February 26, 2019, date of current version March 26, 2019.

Digital Object Identifier 10.1109/ACCESS.2019.2901740

Research on Channel Power Allocation of Fog Wireless Access Network Based on NOMA

WENLE BAI[1,2], TONG YAO[1], HAIJUN ZHANG[3], (Senior Member, IEEE), AND VICTOR C. M. LEUNG[4], (Fellow, IEEE)

[1]School of Electronic and Information Engineering, North China University of Technology, Beijing 100144, China
[2]State Key Laboratory of Network and Switching Technology, Beijing University of Posts and Telecommunications, Beijing 100876, China
[3]Beijing Advanced Innovation Center for Materials Genome Engineering, Beijing Engineering and Technology Research Center for Convergence Networks and Ubiquitous Services, Institute of Artificial Intelligence, University of Science and Technology Beijing, Beijing 100083, China
[4]Department of Electrical and Computer Engineering, The University of British Columbia, Vancouver, BC V6T 1Z4, Canada

Corresponding author: Wenle Bai (bwl@ncut.edu.cn)

This work was supported in part by the National Natural Science Foundation of China under Grant 61371143, in part by the Industrial-University Cooperation and Collaborative Education Project for Higher Education Department of the Ministry of Education under Grant 201801121002, in part by the Project of 2019 for Association of Computing Education in Chinese Universities under Grant CERACU2019R05, and in part by the Open Foundation of the State Key Laboratory of Networking and Switching Technology, Beijing University of Posts and Telecommunications, under Grant SKLNST-2016-2-15.

ABSTRACT With the developing of the smart mobile terminal and wideband application in the mobile Internet, the requirement of large capacity, low latency, and high scalability in the future network is becoming more and more stringent. Edge computing is attracting great attention to decrease time delay and improve the quality of networks' service. By integrating fog computing with the radio access network (RAN) and taking full advantage of the edge computing, fog RAN (F-RAN) is expected as a promising example for 5G/6G systems. The idea of NOMA is to distinguish users whose information is multiplexed into the same orthogonal resource by different power factors, and successive interference cancellation (SIC) is used to detect information at the fog access nodes. In this paper, we focus on dynamic power allocation of wireless sub-channel in NOMA and extend it to F-RAN. A three-user multiplexing model of a NOMA multiuser system model is developed at the transmitting side and the corresponding SIC receiver is designed. Moreover, a group of dynamic power adjusting factors is defined according to users' channel conditions, and an improved fractional transmit power allocation (I-FTPA) algorithm is proposed for NOMA and applied to the three-user model. The experimental results demonstrate that the I-FTPA performs better than the previous FPA and FTPA, more meaningful is that more than one wireless channel power allocation schemes can be found performing better than OFDMA under the same conditions for F-RAN by using the I-FTPA, which provides some significance for deploying NOMA into F-RAN in the future application.

INDEX TERMS Edge computing, F-RAN, NOMA, dynamic power allocation, I-FTPA.

I. INTRODUCTION

In the past few decades of development, explosive growth of wireless communication data has promoted development on the following generation of mobile communication networks (5G). In the future 5G, the three application scenarios: enhanced mobile broadband (eMBB), massive-type communication (mMTC) and ultra-reliable low-latency communications (uRLLC) require the future network to be seamless, stable, low latency and high scalability. These characteristics have promoted the research on novel wireless network architecture and multiple access technology.

A fog computing based on Cloud Radio Access Network (F-RAN) architecture is proposed as a promising access network architecture for the fifth generation of mobile communication to reduce the heavy burden on the capacity-limited front-haul. In [1], the concept of F-RAN is proposed to improve spectral efficiency and energy efficiency of wireless networks by Cisco. In F-RAN, the complicated application demanding intensive computation and high energy consumption attend to computing in cloud center, the application which is sensitive to latency prefer to computing in fog part, providing users with distributed signal processing and computing, which can reduce the signaling overhead in handover process [2]. In other words, a large scale of signal processing is processed in a distributed manner, rather than

The associate editor coordinating the review of this manuscript and approving it for publication was Zhiguo Ding.

being concentrated in building baseband unit (BBU) pool, data is stored in the fog access node (F-AP), UE in F-RAN. The feature of F-RAN is the ability to maximize the usage of network edge devices and reduce latency.

However, the large amount of data of applications would be delivered from the users to the fog access nodes (F-AP)) or cloud center through wireless links, demanding the need for enormous communication bandwidth, which is limited and expensive resource. To improve the efficiency and reduce the latency, NOMA is verified as a promising multiple access mechanism for future RAN to meet the demands for low latency, massive connectivity, and high throughput [3]. The idea of NOMA is to superpose users' information into the same time, frequency and code domain with different power level, and SIC can be applied at the fog access node (F-AP) for separating different users' signals.

A common fact is that the fog access nodes (F-AP) usually do not have enough storage capacity and computing resources and may not meet large-scale users' services, therefore, the implementation scheme of NOMA will have great impact on F-RAN. There are lots of researches about NOMA and F-RAN. [4] Zhang *et al.* [4] propose the fog radio access networks based on NOMA and corresponding resource management mechanisms to reduce delay and improve quality of service (QoS) for networks. Chunlin *et al.* [5] innovatively advocate a design scheme for the transmitter and receiver of NOMA system. The proposed scheme can reach a good performance as codeword-level SIC (CWIC) does even when power ratio is approximate between cell center user and edge user, but with low complexity. In [6], an iterative multiuser detection and decoding (MUDD) method are proposed to optimize receiver performance, which brings about 4.6dB (QPSK) and 9.8dB (16QAM) performance gain at block error rate (BLER) compared to the traditional multiuser detection. Reference [7] presents the influence of error vector magnitude (EVM) to different SIC in downlink NOMA receivers' accuracy. When EVM is NOMA is 4% and power allocated to cell center user ranges from 0.2 to 0.37, simulations show that its performance is almost the same as OFDMA. In [8], performance and design of NOMA-SIC receiver based on 2*2 SU-MIMO are studied. To reduce inference of both inter-user and inter-stream at receiver, it introduces different weight generation schemes according to the combination of transmission ranks between UEs, and compares BLERs of various SIC receivers under different transmit powers, rank combinations, modulation and coding schemes (MCS). Benjebbour *et al.* [9] propose the error propagation model of SIC receiver design in NOMA and a worst case model is considered and researched. The experimental results show that under wide-band/sub-band scheduling and low/high mobility scenarios, NOMA can still receive its expected gains regardless of error propagation.

Although a lot of related works have integrated F-RAN with NOMA techniques and many resource allocation scheme are developed efficiently, almost all researches on wireless channel power allocation are fixed power allocation under specific channel conditions, which can not effectively adapt to the changes of channel conditions in practice. Inspired by this, this paper proposes a dynamic channel resource allocation scheme to adapt to changes of channel conditions and extend to F-RAN: I-FTPA, whose performance is researched and compared with traditional OFDMA, NOMA-FPA and NOMA-FTPA.

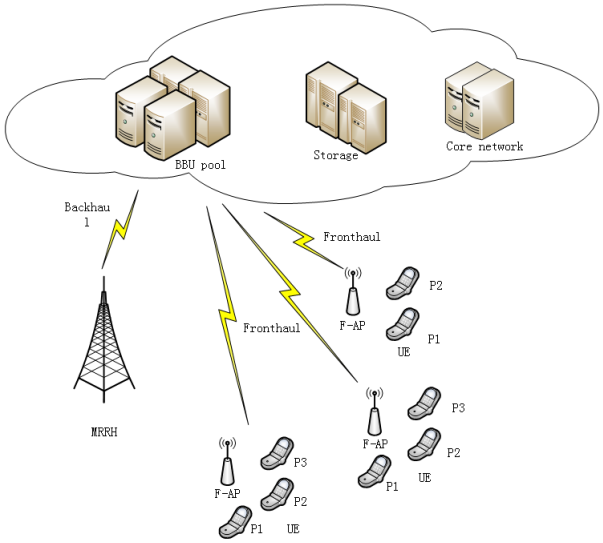

FIGURE 1. Structure of NOMA-Based F-RAN.

The rest of paper is organized as follows. Section II describes system model. Different power allocation algorithms are introduced and I-FTPA is proposed in section III. In section IV, the mentioned power allocation algorithms are simulated and corresponding results are analyzed. Finally, section V concludes the paper.

II. SYSTEM MODEL

A. FOG RADIO ACCESS NETWORK BASED ON NOMA

Fig. 1 shows the structure of F-RAN Based on NOMA. In this structure, the part of computing, storage, control and management are integrated into the macro remote heads (MRRH) and fog access nodes (F-AP) at the edge of the network. BBU pool provides the centralized storage and communication. The MRRH is connected to the BBU through the backhaul link, and the fog access nodes are connected to the BBU through the fronthaul link. Each user equipment (UE) with different allocated power using NOMA is connected to the F-AP. And the detailed structure of NOMA multiuser is shown in Fig. 2, where UE-1 is a central user, UE-2 is an intermediate user and UE-3 is an edge user. The transmitted signal of UE-i (i = 1, 2, 3) is x_i, and signal power allocated to each user is P_i. According to the power allocation principle in NOMA [12], since UE-3 has the lowest SINR, it is assigned a larger power, UE-2's SINR is moderate among three users, a moderate power is assigned, and for UE-1, as it has a better SINR, a minimum power is allocated.

The transmitted signal superposed in power domain can be expressed as:

$$X = \sqrt{P_1}d(x_1) + \sqrt{P_2}d(x_2) + \sqrt{P_3}d(x_3) \quad (1)$$

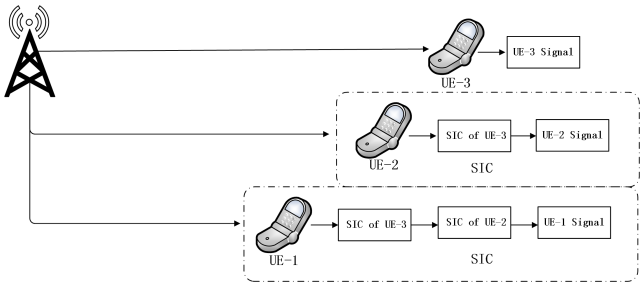

FIGURE 2. Structure of NOMA multiuser system.

where $d(x_1)$, $d(x_2)$ and $d(x_3)$ represent the modulation and channel coding for original UEs' signals. The sum power of 3 users follows the constraint as:

$$P = P_1 + P_2 + P_3 \tag{2}$$

in which P = 1. The received signal of UE-i is:

$$Y_i = h_i \left(\sqrt{P_1} d\,(x_1) + \sqrt{P_2} d\,(x_2) + \sqrt{P_3} d\,(x_3) \right) + \omega_i \tag{3}$$

where h_i is complex channel coefficient between UE-i and base station (BS), as for ω_i, additive white Gaussian noise. The power-spectral density of ω_i denotes $N_{0,i}$.

From the above, process of multiplexing 3 users information into one resource block in NOMA is presented. To detect them and separate their own information, we design a 3-users code-word level SIC receiver in the following section.

B. SIC RECEIVER

For SIC receiver, it first sorts each user according to channel gain, i.e. $|h_i|^2/N_{0,i}$, in descending order. In 3-users NOMA, the channel gain satisfies the following condition: $|h_i|^2/N_{0,i} < |h_j|^2/N_{0,j} < |h_k|^2/N_{0,k}$. At UE-i side, signal of UE-i is directly demodulated and decoded while regarding UE-j and UE-k as an interference; at UE-j side, the UE-i signal is first detected and removed from the received signal by SIC to detect UE-j signal; as for UE-k, signals of UE-i and UE-j are first detected and then removed by SIC, then what is left is signal of UE-k.

Fig. 3 shows structure of symbol level SIC (SLIC) and code-word level SIC (CWIC). The main difference is that CWIC includes the process of demodulation and channel decoding, while SLIC does not, which indicates that CWIC may decrease the error propagation at the cost of complexity. In our work, CWIC receiver is adopted for better performance of the system. Fig. 4 demonstrates CWIC receiver of 3 users.

In Fig. 4, UE-3 is an edge user. It has the largest allocated power than other two users, which can make sure that this user can directly detect its information by treating others' as noise in the process of detecting and receiving signal of itself. The final signal can be expressed as:

$$\hat{X}_3 = \left\lfloor \frac{Y_3}{\sqrt{P_3}} \right\rfloor \tag{4}$$

where $\lfloor . \rfloor$ represents demodulation and channel decoding process. At UE-2 received end, after removing UE-3's signal

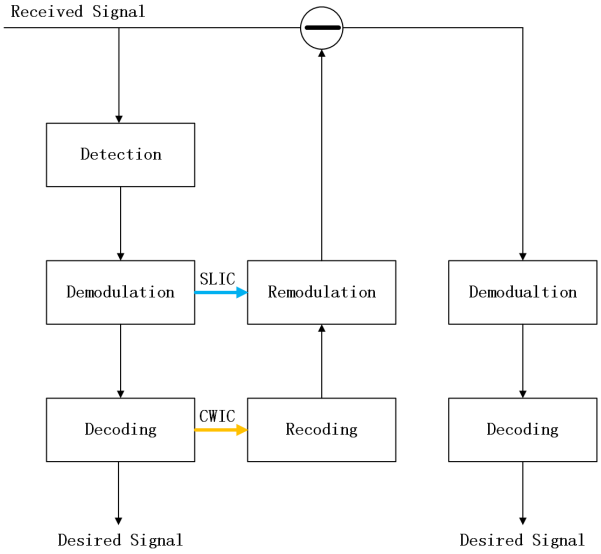

FIGURE 3. SLIC & CWIC.

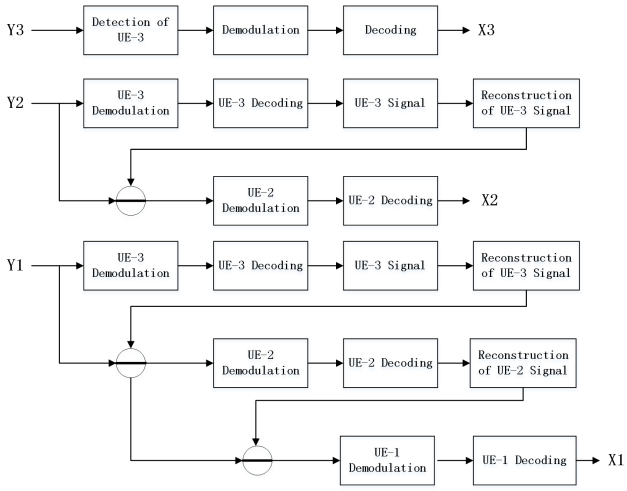

FIGURE 4. Code-word level SIC receiver of 3 users.

from received signal by SIC, UE-2's signal is:

$$\hat{X}_2 = \left\lfloor \frac{Y_2 - \sqrt{P_3} \left\langle \hat{X}_3 \right\rangle}{\sqrt{P_2}} \right\rfloor \tag{5}$$

$\langle . \rangle$ represents the modulation and channel coding process. At UE-1 receiver, the interference of UE-3 and UE-2's signals are eliminated by SIC. Finally, UE-1's signal is represented as:

$$\hat{X}_1 = \left\lfloor \frac{Y_1 - \sqrt{P_2} \left\langle \hat{X}_2 \right\rangle - \sqrt{P_3} \left\langle \hat{X}_3 \right\rangle}{\sqrt{P_1}} \right\rfloor \tag{6}$$

according to [9], SINR of UE-i after SIC is illustrated as:

$$SINR(UE - i) = \frac{|h_i|^2 P_i}{\left(\sum\limits_{\frac{|h_i|^2}{N_{0,i}} < \frac{|h_j|^2}{N_{0,j}}} |h_i|^2 P_j + N_{0,i} \right)} \tag{7}$$

then SINRs of 3-users NOMA system are shown as follow:

$$SINR(UE-3)=\frac{|h_3|^2P_3}{|h_3|^2P_1+|h_3|^2P_2+N_{0,3}} \quad (8)$$

$$SINR(UE-2)=\frac{|h_2|^2P_2}{|h_2|^2P_1+N_{0,2}} \quad (9)$$

$$SINR(UE-1)=\frac{|h_1|^2P_1}{N_{0,1}} \quad (10)$$

III. POWER ALLOCATION ALGORITHMS

From (4), (5), (6), (7), (8), (9) and (10), we find that power allocated to different UE influences restoration of signals, SINRs and final accuracy of signal detection at received ends of NOMA. In order to adapt to changes in channel conditions for NOMA application, we explore different power allocation schemes, moreover, propose an I-FTPA scheme.

A. FPA

For fixed power allocation (FPA), each user power is assigned a different fixed power by its channel gain, that is, user of poor channel gain, a larger power is assigned (e.g. 0.6 P), for users with a good channel gain, a large power is assigned (e.g. 0.3P), and user of better channel gain is assigned a small power (e.g. 0.1 P). FPA is the simplest algorithm, which can reduce the signaling overhead between BS and UE significantly, but it is too rough. The big problem of FPA is that it does not have a specific power allocation formula to calculate how much power should be allocated to different user based on its' channel gain, which means the simple criterion that it use can not determine whether this power matches current channel condition or not. Further, it also cannot perform power allocation according to channel fluctuation.

B. I-FTPA

Aimed at solving the above problem in FPA, based on fractional transmitted power allocation (FTPA) scheme studied in [9], we propose an Improved Fractional Transmit Power Allocation (I-FTPA) algorithm. Compared to FTPA, which has only a single decay factor for power adjustment, I-FTPA has different varying decay factor to adjust each user's channel gain, Which provides convenient to adjust transmitted power according to channel changes automatically. The value of varying decay factor is between 0 and 1. In I-FTPA, power allocated to each UE-i is defined by (11):

$$P_i=\left(\frac{P}{\left(|h_1|^2/N_{0.1}\right)^{-\beta_1}+\ldots+\left(|h_i|^2/N_{0.i}\right)^{-\beta_i}}\right)*\left(|h_i|^2/N_{0.i}\right)^{-\beta_i},\quad i\in U_s \quad (11)$$

In which different β_i can adjust the channel gain of different users, this enables the final assigned power of each user to change accordingly with channel gains. And U_s represents users' set and allocated power for each user follows that $\sum P_i=1, i\in U_s$.

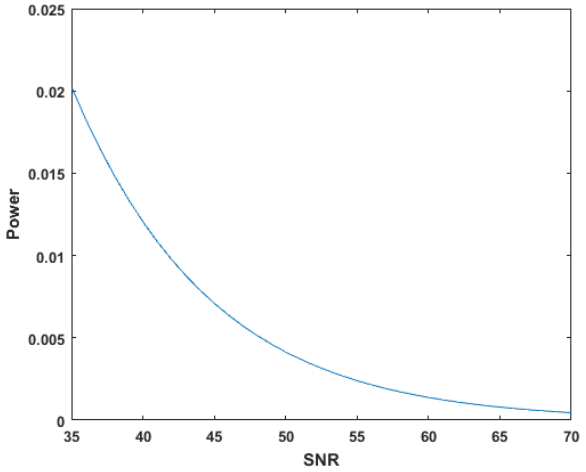

FIGURE 5. Allocated power for UE-1 using I-FTPA, $\beta_1=0.6, \beta_2=0.3, \beta_3=0.1$.

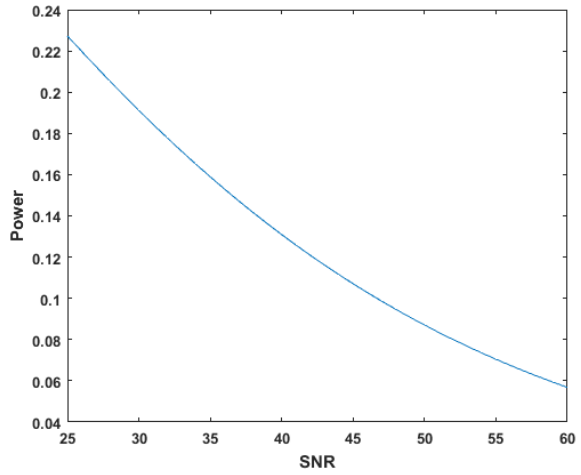

FIGURE 6. Allocated power for UE-2 using I-FTPA, $\beta_1=0.6, \beta_2=0.3, \beta_3=0.1$.

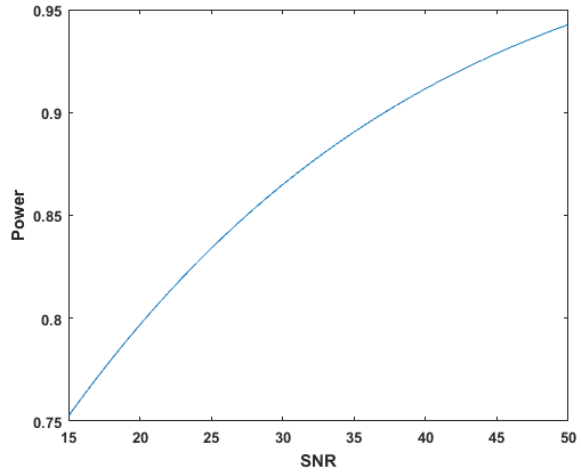

FIGURE 7. Allocated power for UE-3 using I-FTPA, $\beta_1=0.6, \beta_2=0.3, \beta_3=0.1$.

We use (11) to calculate each user's allocated power, and the varying decay factor of UE-1, UE-2 and UE-3 in I-FTPA is: 0.6, 0.3 and 0.1 respectively. Fig 5, Fig 6 and Fig 7 show

TABLE 1. Power factors for uses when using FTPA.

Single Decay Factor	0.2	0.4	0.6	0.8	1
P_1	0.2748	0.2227	0.1778	0.1400	0.1090
P_2	0.3459	0.3530	0.3547	0.3517	0.3447
P_3	0.3793	0.4243	0.4676	0.5083	0.5463

TABLE 2. Power factors for uses when using I-FTPA.

Varying Decay Factor	$\beta_1 = 0.6, \beta_2 = 0.3, \beta_3 = 0.1$				
SNR(dB)	20	30	40	50	60
P_1	0.0668	0.0247	0.0086	0.0029	0.0009
P_2	0.2657	0.1958	0.1356	0.0906	0.0593
P_3	0.6675	0.7795	0.8558	0.9065	0.9389

TABLE 3. Simulation parameters.

Radio Access Scheme	OFDM
Modulation	NOMA:QPSK OFDM:64PSK
Antenna Configuration	BS:1Tx UE:1Rx
Channel Coding/Decoding	Turbo
Channel Model	AWGN
Channel Estimation	Ideal
FFT Timing Detection	Ideal
Number of Subcarriers	64
OFDM Cyclic Prefix	16
Receiver	Ideal Code-word Level SIC
Number of Multiplexed UEs	1 (OFDMA),3 (NOMA)
NOMA Users Power Allocation Schemes	FPA,FTPA,I-FTPA

the power varying of each user as SNR change. The power allocated for each user still follows the principle that their sum is 1, and user with better channel conditions is allocated small power, and user with poor channel conditions is allocated large power. As for FTPA, when the single decay factor is fixed, the power assigned to each user remains unchanged for each user, regardless of how the SNR changes. Table 1 and Table 2 shows the different power allocation schemes for each user when single decay factor varies in FTPA and varying decay factors varies in I-FTPA, respectively. From it, we can learn that power for each user only change when single decay factor alters in FTPA. From the comparison of these two algorithms, we can see that I-FTPA may have more power allocation schemes with a group of decay factors according to the demanding of channel varying than FTPA.

IV. SIMULATION EVALUATIONS

In this section, we evaluate the performance of the proposed I-FTPA, we implement the system simulation by comparing BER performance according to the parameters as shown in Table 3 and simulation block diagram as shown in Fig. 8. First, we compare BER performance of NOMA and OFDMA under same transmitted bits, i.e. each user in NOMA adopts QPSK modulation, respectively, while OFDMA user is modulated by 64PSK. Moreover the BER performance between FPA and I-FTPA is compared and analyzed.

In Figs. 9 and 10, we compare NOMA-QPSK with OFDMA-64PSK when adapting I-FTPA under different power allocation schemes. In Fig. 9 ($\beta_1 = 0.6, \beta_2 = 0.35, \beta_3 = 0.05$), when energy per bit to noise power spectral density ratio (Eb/N0) is almost 20dB, bit error rates (BERs) of NOMA UE-1, NOMA UE-2 and NOMA UE-3 are $10^{-3.076}$, $10^{-2.167}$ and $10^{-0.483}$, respectively, compared to $10^{-0.320}$ of OFDMA UE. In Fig. 10 ($\beta_1 = 0.7, \beta_2 = 0.25, \beta_3 = 0.05$), when Eb/N0 is almost 20dB with another group of decay factors, BERs of NOMA UE-1, NOMA UE-2 and NOMA UE-3 are $10^{-3.521}$, $10^{-3.073}$ and $10^{-0.350}$, separately, with the comparison of $10^{-0.320}$ of OFDMA UE.

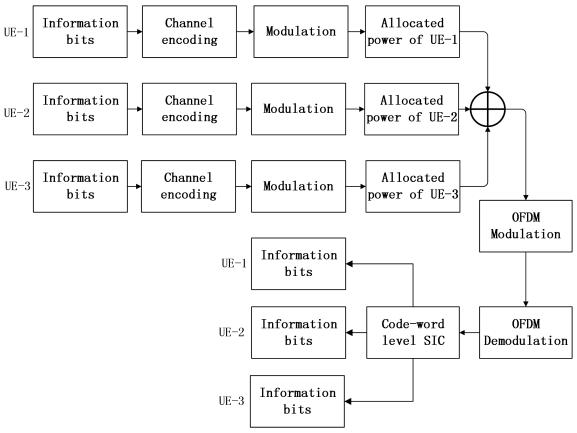

FIGURE 8. System simulation block diagram.

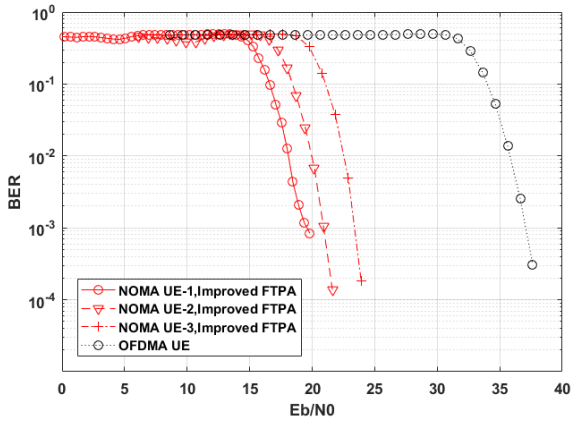

FIGURE 9. NOMA-QPSK VS OFDMA-64PSK, $\beta_1 = 0.6, \beta_2 = 0.35, \beta_3 = 0.05$.

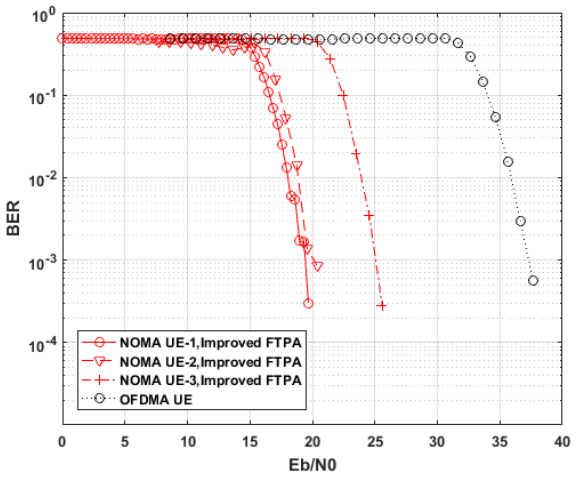

FIGURE 10. NOMA-QPSK VS OFDMA-64PSK, $\beta_1 = 0.7, \beta_2 = 0.25, \beta_3 = 0.05$.

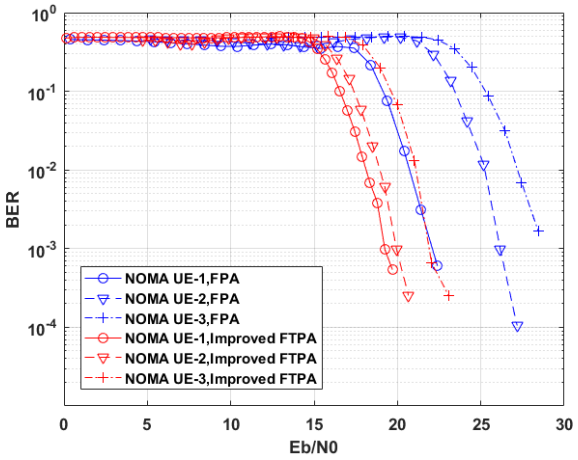

FIGURE 11. BER performance of NOMA FPA VS NOMA improved FTPA.

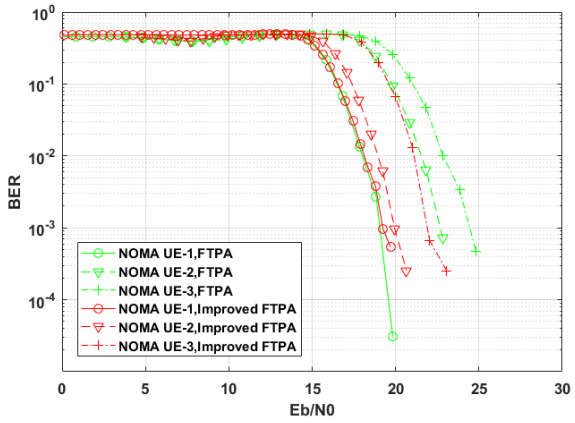

FIGURE 12. BER performance of NOMA FTPA VS NOMA improved FTPA.

From the above two simulation results, it can be found that all of NOMA UEs gradually outperform OFDMA UE as Eb/N0 increases. In both two power allocation situations, when Eb/N0 exceeds about 15dB, BERs of NOMA UE-1 and UE-2 are almost lower than OFDMA UE, and for NOMA UE-3, it outperforms OFDMA UE when Eb/N0 nearly surpasses 20dB, all three users performs much better than that of OFDMA.

It can also be seen that different varying decay factors of I-FTPA have unequal influence in NOMA. In Fig. 9, NOMA UE-3 outperforms UE-3 of Fig. 10, whereas BER performances of NOMA UE-1 and UE-2 are worse than those in Fig. 10. This result means that we can utilize different power distribution schemes according to practical application scenarios. From another perspective, we can find more better schemes than OFDMA by using I-FTPA in application scenarios.

Fig. 11 shows BER performance of NOMA FPA VS NOMA I-FTPA. In FPA, power factors assigned to 3 NOMA users are: $P_1 = 0.05, P_2 = 0.15, P_3 = 0.8$, respectively, and in I-FTPA, varying decay factor of each user is $\beta_1 = 0.6, \beta_2 = 0.35, \beta_3 = 0.05$, separately. When Eb/N0 reaches nearly 20dB, BERs of UE-3 using FPA and I-FTPA are $10^{-0.305}$, $10^{-1.173}$; BERs of UE-2 with FPA and I-FTPA can be expressed as $10^{-0.311}$, $10^{-3.011}$; BERs of UE-1 in FPA and I-FTPA are $10^{-1.760}$, $10^{-3.269}$. It can also be seen that as Eb/N0 increases, BER performance of NOMA I-FTPA totally outperforms that of NOMA FPA.

In Fig.12, BER performance of NOMA FTPA VS NOMA I-FTPA is illustrated. The single decay factor is 0.9 in FTPA. And in I-FTPA, the varying decay factor of each user is the same as Fig.7 ($\beta_1 = 0.6, \beta_2 = 0.35, \beta_3 = 0.05$). When Eb/N0 reaches nearly 20dB, BERs of UE-3 with FTPA and I-FTPA are $10^{-0.587}$, $10^{-1.173}$; BERs of UE-2 can be expressed as $10^{-1.023}$ and $10^{-3.011}$. As for UE-1, the curve of I-FTPA is approximately coincident with that of FTPA. The above results illustrate that overall system performance of NOMA I-FTPA is still relatively better than that of NOMA-FTPA.

As seem from the above, we can find more than one power allocation schemes of NOMA outperforming OFDMA under the same circumstances through I-FTPA. Different varying decay factors of I-FTPA also have different influence on 3 users' final detection accuracy, which can be changed to meet the need of each user under different applications. Also, I-FTPA performs better than that of FPA and FTPA in NOMA.

V. SUMMARY

In this paper, we extend NOMA to F-RAN and present a model with 3 users multiplexed at transmitter, and corresponding receiver design. To further improve adaptability to channel conditions, we then proposes a dynamical resource allocation scheme for NOMA: I-FTPA. It is constructed by defining multiple varying decay factors. Simulation results demonstrate the effectiveness of several resource allocation schemes. By comparison, I-FTPA is better than the previous FPA and FTPA, a meaningful discovery is that more than one wireless channel power allocation schemes can be found performing better than OFDMA under same conditions for F-RAN by using I-FTPA, which provide some theory basis for integrating NOMA with F-RAN in the future application.

REFERENCES

[1] F. Bonomi, R. Milito, J. Zhu, and S. Addepalli, "Fog computing and its role in the Internet of Things," in *Proc. ACM SIGCOMM*, 2012, pp. 13–16.
[2] H. Zhang, Y. Qiu, X. Chu, K. Long, and V. C. M. Leung, "Fog radio access networks: Mobility management, interference mitigation, and resource optimization," *IEEE Wireless Commun.*, vol. 24, no. 6, pp. 120–127, Dec. 2017.
[3] Y. Wang, B. Ren, S. Sun, S. Kang, and X. Yue, "Analysis of non-orthogonal multiple access for 5G," *China Commun.*, vol. 13, no. 2, pp. 52–66, 2016.
[4] H. Zhang, Y. Qiu, K. Long, G. K. Karagiannidis, X. Wang, and A. Nallanathan, "Resource allocation in NOMA-based fog radio access networks," *IEEE Wireless Commun.*, vol. 25, no. 3, pp. 110–115, Jun. 2018.
[5] C. Yan, A. Harada, A. Benjebbour, Y. Lan, A. Li, and H. Jiang, "Receiver design for downlink non-orthogonal multiple access (NOMA)," in *Proc. IEEE 81st Veh. Technol. Conf. (VTC)*, May 2015, pp. 1–6.
[6] M. Al-Imari, P. Xiao, and M. A. Imran, "Receiver and resource allocation optimization for uplink NOMA in 5G wireless networks," in *Proc. Int. Symp. Wireless Commun. Syst. (ISWCS)*, Aug. 2015, pp. 151–155.

[7] K. Saito, A. Benjebbour, A. Harada, Y. Kishiyama, and T. Nakamura, "Link-level performance of downlink NOMA with SIC receiver considering error vector magnitude," in *Proc. IEEE 81st Veh. Technol. Conf. (VTC)*, May 2015, pp. 1–5.
[8] K. Saito, A. Benjebbour, Y. Kishiyama, Y. Okumura, and T. Nakamura, "Performance and design of SIC receiver for downlink NOMA with open-loop SU-MIMO," in *Proc. IEEE Int. Conf. Commun. Workshop (ICCW)*, Jun. 2015, pp. 1161–1165.
[9] A. Benjebbovu, A. Li, Y. Saito, Y. Kishiyama, A. Harada, and T. Nakamura, "System-level performance of downlink NOMA for future LTE enhancements," in *Proc. IEEE Globecom Workshops (GC Wkshps)*, Dec. 2013, pp. 66–70.
[10] *Evolved Universal Terrestrial Radio Access (E-UTRA) and Evolved Universal Terrestrial Radio Access Network (E-UTRAN); Overall Description*, document TS36.300, 3GPP, 2010.
[11] D. Tse and P. Viswanath, *Fundamentals of Wireless Communication*. Cambridge, U.K.: Cambridge Univ. Press, 2005.
[12] F.-L. Luo and C. Zhang, *Signal Processing for 5G: Algorithms and Implementations*. Hoboken, NJ, USA: Wiley, 2016.
[13] S. Gollakota, S. D. Perli, and D. Katabi, "Interference alignment and cancellation," *ACM SIGCOMM Comput. Commun. Rev.*, vol. 39, no. 4, pp. 159–170, 2009.
[14] A. Osseiran, J. F. Monserrat, P. Marsch, M. Dohler, and T. Nakamura, *5G Mobile and Wireless Communications Technology*. Cambridge, U.K.: Cambridge Univ. Press, 2016.
[15] *Evolved Universal Terrestrial Radio Access (E-UTRA), Physical Layer Procedures*, document TS 36.213 V12.5.0, 3GPP, 2015.

WENLE BAI was born in Shanxi, China, in 1967. He received the Ph.D. degree in communication engineering from the Beijing University of Posts and Telecommunication of China, in 2006. He is currently an Associate Professor with the North China University of Technology. His research interests include wireless communications, statistical signal processing, and multi-user communication. He has published about 20 papers in the related areas.

TONG YAO was born in Beijing, China. He received the B.E. degree in electrical engineering from the North China University of Technology, in 2012, where he is currently pursuing the M.E. degree in information and communication engineering. His research interests include wireless networks and wireless communications.

HAIJUN ZHANG (M'13–SM'17) is currently a Full Professor with the University of Science and Technology Beijing, China. He serves as an Editor for the IEEE TRANSACTIONS ON COMMUNICATIONS, the IEEE TRANSACTIONS ON GREEN COMMUNICATIONS NETWORKING, and the IEEE COMMUNICATIONS LETTERS.

VICTOR C. M. LEUNG (S'75–M'89–SM'7–F'03) received the B.A.Sc. degree (Hons.) in electrical engineering from The University of British Columbia (UBC), in 1977, and the Ph.D. degree in electrical engineering from UBC, in 1982. He attended the Graduate School at UBC on a Natural Sciences and Engineering Research Council Postgraduate Scholarship. From 1981 to 1987, he was a Senior Member of the Technical Staff with Microtel Pacific Research Ltd., (later renamed MPR Teltech Ltd.), Burnaby, Canada, where he specialized in the planning, design, and analysis of satellite communication systems. He also held a part-time position as a Visiting Assistant Professor with Simon Fraser University, in 1986 and 1987, respectively. In 1988, he was a Lecturer with the Department of Electronics, The Chinese University of Hong Kong. He returned to UBC as a Faculty Member, in 1989, where he is currently a Professor and the inaugural holder of the TELUS Mobility Industrial Research Chair in advanced telecommunications engineering with the Department of Electrical and Computer Engineering. He is also the Director of the Laboratory for Wireless Networks and Mobile Systems (WiNMoS) and a member of the Institute for Computing, Information and Cognitive Systems, UBC He also holds or has held Guest/Adjunct Professor appointments with Jilin University, Beijing Jiaotong University, South China University of Technology, The Hong Kong Polytechnic University, Beijing University of Posts and Telecommunications, and Hefei University of Technology. He has authored/co-authored over 1100 papers in archival journals and international conferences, as well as 40 book chapters. He has also co-authored/co-edited 14 books. His research interests are in the broad areas of wireless networks and mobile systems. He is a registered member of the Engineers and Geoscientists BC, Canada. He is a Fellow of the Academy of Science, Royal Society of Canada; a Fellow of the Engineering Institute of Canada; a Fellow of the Canadian Academy of Engineering; and a Voting Member of the ACM. He has guest-edited many special journal issues, and has served on the Technical Program Committee of numerous international conferences. He has provided leadership to the Technical Program Committees and Organization Committees of many international conferences. He was a recipient of the 2011 UBC Killam Research Prize, the IEEE Vancouver Section Centennial Award and the 2017 Canadian Award for Telecommunications Research, and the 2018 IEEE ComSoc TGCC Distinguished Technical Achievement Recognition Award. He has co-authored papers that won the 2017 IEEE ComSoc Fred W. Ellersick Prize, the 2017 IEEE Systems Journal Best Paper Award, and the 2018 IEEE ComSoc CSIM Best Journal Paper Award. He was awarded the APEBC Gold Medal as the Head of the Graduating Class in the Faculty of Applied Science, UBC. He is serving on the Editorial Boards of the IEEE TRANSACTIONS ON GREEN COMMUNICATIONS AND NETWORKING, the IEEE TRANSACTIONS ON CLOUD COMPUTING, the IEEE ACCESS, the *Computer Communications*, and several other journals. He has previously served on the Editorial Boards of the IEEE JOURNAL ON SELECTED AREAS IN COMMUNICATIONS (Wireless Communications Series and Series on Green Communications and Networking), the IEEE TRANSACTIONS ON WIRELESS COMMUNICATIONS, the IEEE TRANSACTIONS ON COMPUTERS, the IEEE TRANSACTIONS ON VEHICULAR TECHNOLOGY, the IEEE WIRELESS COMMUNICATIONS LETTERS, and the *Journal of Communications and Networks*. He was a Distinguished Lecturer of the IEEE Communications Society, from 2009 to 2012.